Near-zero energy proton production mechanisms from the three-body dissociation of H_3^+

O. Yenen, L. M. Wiese, D. Calabrese, and D. H. Jaecks
Behlen Laboratory of Physics, University of Nebraska, Lincoln, Nebraska 68588-0111
(Received 27 December 1989)

The laboratory energy distribution of H^+ from the dissociation of H_3^+ in low-keV H_3^+-He collisions is measured at a 0° laboratory angle. An inelastic energy loss of $Q=26\pm2$ eV has been determined for the excited states of H_3^+ that produce low-energy protons upon dissociation. An approximate projectile-frame energy distribution of H^+ is also presented. Our results suggest that the near-zero projectile-frame energy protons are produced by either an electronic singlet excitation of the ground state of H_3^+ to a distribution of $2\,^1E'$, $1\,^1E''$, and $2\,^1A_2''$, or as an alternative mechanism, a triplet excitation of H_3^+ to $1\,^3E'$ accompanied by a simultaneous triplet excitation of the He target. In either case, the near-zero energy protons are produced by a three-body dissociation of the excited $(H_3^+)^*$. In the case of the triplet excitation, there are no long-range correlations for the motion of the neutral H atoms. For the singlet excitation, the neutral H atoms' motion is correlated and the angle between them is near 180°. The effects of the long-range nature of the total potential between the fragments is discussed in terms of the hyperspherical coordinates.

I. INTRODUCTION

The fundamental nature of the few-body problem spreads across the borders of many disciplines of physics, and its simplest form, the three-body problem, presents many challenges from celestial mechanics to nuclear physics. The three-body problem has been extensively studied both experimentally and theoretically in atomic and molecular physics, when the interaction between the three particles is the Coulomb potential. Specifically, the predictions of Wannier theory,[1] originally derived for the threshold ionization of atoms by electrons, have been experimentally verified.[2] More recently the Wannier theory has been extended to three-particle systems of arbitrary masses interacting through pure Coulomb potentials.[3,4] Even in the case of arbitrary masses, the theory predicts that the correlation angle, i.e., the angle between the two particles of same charge, is 180°. The polar dissociation of H_3^+ into $H^+ + H^+ + H^-$ has been shown to be a good system to study in order to test these predictions. Using the laboratory energy distribution of H^- obtained from the polar dissociation of H_3^+, we were able to set a lower limit of 163° on the correlation angle between the two protons in the center of mass (c.m.) of the dissociating H_3^+.[5] Despite all this progress, many aspects of the three-body problem remain unsolved. The aim of this paper is to experimentally investigate a case when the three particles interact through an atomic interaction other than the pure Coulomb potential by using the laboratory energy distribution of protons obtained from the dissociation of H_3^+ colliding with a He target at low-keV energies. The two previously published measurements of the laboratory H^+ energy spectra[6,7] that we are aware of do not have sufficient resolution to accurately determine the inelastic energy loss or separate various parts of the energy spectra.

II. EXPERIMENT AND RESULTS

We have measured the laboratory energy distribution of protons emitted at 0° from the collision-induced dissociation of H_3^+. The experimental setup is essentially the same as the earlier experiment we have performed to measure the laboratory energy spectrum of H^- produced by the three-body dissociation channel, $H^+ + H^+ + H^-$ of H_3^+.[5] Briefly, the H_3^+ ions from a dupolasmatron source are accelerated to low-keV energies, mass selected by an analyzing magnet, and focused. This H_3^+ beam collides under single-collision conditions with the target gas (He) in a small cell, and the dissociation products proceed to a parallel plate energy analyzer with a 0.27% full width at half maximum (FWHM) energy resolution. The unused portion of the beam passes through high transmission wire meshes at the middle and the back plates, and is collected in a Faraday cup. The protons from the H_3^+ dissociation are detected by a discrete-anode position sensitive detector utilizing a pair of microchannel plates (MCP's) in chevron configuration. The finite size of the beam and the anodes of the MCP's limit the determination of the beam direction to 0 ± 0.03°. The proton counts are normalized to Ly-α photon counts from the collision cell that are simultaneously monitored by a solar-blind photomultiplier to account for small fluctuations in the beam current and/or target gas pressure. Figure 1 schematically shows the experimental setup. The data collection electronics is the same as previously described.[5] We have used the three pins at 0° to obtain three simultaneous laboratory proton spectra for a given beam energy and repeated the process many times at several incoming beam energies ranging from 4.0 to 7.0 keV. A step size of approximately 1.5 eV (1 V of analyzer voltage) is used. In a typical raw spectrum, the positively charged particle background and the dark counts of the

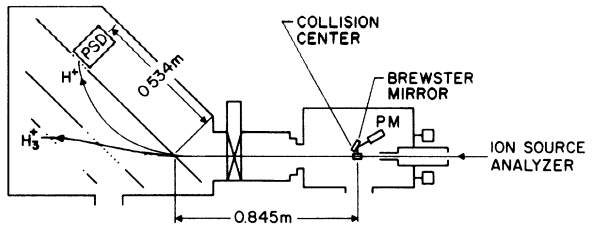

FIG. 1. Schematic experimental setup. The multipin position-sensitive detector (PSD) and the solar-blind photomultiplier (PM) used to simultaneously monitor the Ly-α photons, are shown.

MCP's being less than 0.01% of the maximum count rate, no background subtraction is performed. Several spectra taken at 4.0, 4.5, 5.0, 5.5, 6.0, 6.5, and 7.0 keV did not show any variations from those at 4.0 and 4.5 keV shown in Fig. 2.

Although the importance of the molecular c.m. deflection after electronic excitation in H_3^+-He collisions at low-keV energies is not well established, it is possible to gain some insight by considering the c.m. deflection of H_2^+ in low-keV H_2^+-He collisions. Meierjohann and Vogler[8] have experimentally shown that the electronic excitation of H_2^+ in H_2^+-He collisions at 10 keV occurs for a c.m. deflection of less than 0.1°. Similarly, Baldreich, Lotz, and Ewald[9] experimentally determined that the dissociative electronic excitations of H_2^+ result from processes without the deflection of the c.m. of H_2^+. They also concluded that the dissociative vibrational excitations of H_2^+ result in significant c.m. deflections. Therefore it is reasonable to assume that with the exception of dissociations due to violent collisions of the nuclei, the momentum transfer between H_3^+ and He is small and the deflection of the c.m. of H_3^+ is negligible to a good approximation.

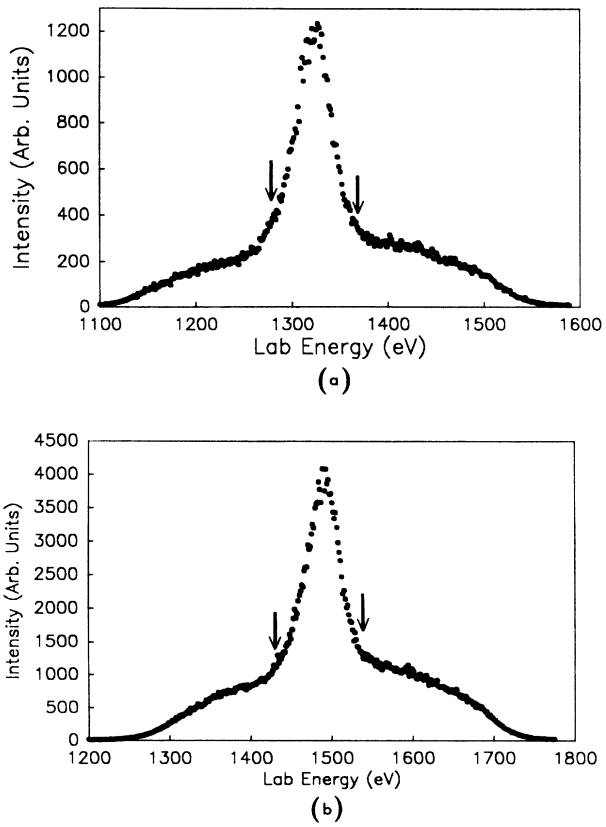

FIG. 2. Laboratory energy distribution of protons at 0° from the collision induced dissociation of (a) 4.0-keV, (b) 4.5-keV H_3^+ ions on He targets. Several spectra, taken at incoming beam energies ranging from 4.0 to 7.0 keV, did not show any significant change from the ones presented.

Under these conditions, the interpretation of fragment laboratory energy spectra was explained in detail in our previous publication.[5] Briefly, the incoming H_3^+ ion of energy E_0 collides with the He target and is excited to a dissociative state while slowing down to provide this excitation energy. Thus, after the collision, the center of mass of the dissociating $(H_3^+)^*$ moves with an energy E_0-Q, where Q is the inelastic energy loss. Upon dissociation, the potential energy of the excited H_3^+, above the dissociation limit, is transformed into the kinetic energy of the fragments in the c.m. of H_3^+. The velocity of a fragment in the laboratory frame is the vector sum of the velocity of the c.m. of H_3^+ after the collision and the velocity of the fragment in the projectile frame. When the measurement is made at a 0° laboratory angle, we obtain the following relations:

$$E_{\rm lab}=\tfrac{1}{2}m(V\pm v)^2\ , \tag{1}$$

$$E_{\rm lab}=(E_0-Q)/3+\varepsilon_+\pm 2[(\varepsilon_+)(E_0-Q)/3]^{1/2}\ , \tag{2}$$

where m is the mass of the proton; v and ε_+ its speed and kinetic energy, respectively, in the c.m. of dissociating H_3^+; and V is the speed of the c.m. of H_3^+ immediately after the collision. The Newton diagram of a process which produces a proton at a 0° laboratory angle and two neutral hydrogen atoms is shown in Fig. 3. This method provides a sensitive way of measuring the energy spectrum because of the plus or minus term in Eq. (2), which serves as an amplification factor for the c.m. energies.

As one can see from Eq. (2), if a fragment has near-zero projectile-frame energies, then it will have a unique laboratory-frame energy. Otherwise, it will have two different laboratory energies corresponding to fragments moving forward or backward with respect to the direc-

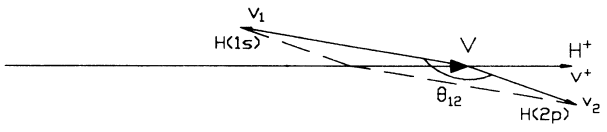

FIG. 3. Newton diagram of the dissociation of H_3^- into $H^+ + H(1s) + H(2p)$. V is the velocity of the center of mass (c.m.) of H_3^+ right after the collision, v^+ the c.m. velocity of the proton, and v_1 and v_2 the c.m. velocities of the neutral H atoms. θ_{12} is the correlation angle between the two H atoms.

tion of the c.m. of the parent molecule. Thus we conclude that any single feature on the laboratory energy distribution of a fragment has to originate from near-zero projectile-frame energy particles. An inspection of the laboratory energy distribution of H^+, presented in Fig. 2, reveals that there is indeed a single peak in addition to the two broad wings on either side of the single peak. The broad wings, known to mass spectroscopists as Aston bands, are due to protons moving forward or backward in the projectile frame. The central peak is due to protons having near-zero velocities in the c.m. of H_3^+. It is easy to see from Eq. (2) that the central peak occurs at a laboratory energy of $(E_0-Q)/3$. Thus the shift of the central peak from $E_0/3$ is a direct measurement of the inelastic energy loss Q of the protons having near-zero energies in the projectile frame. In practice we do not rely on a single datum point; instead we determine the center of the full peak which is shown between the two arrows in Fig. 2. After careful calibration of all power supplies and voltmeters with respect to Valhalla Scientific Model 4500 HV Digital Voltmeter that we use to monitor the accelerating voltage (between the source and the chamber ground), we find that $Q=26\pm2$ eV. When we substitute this value for Q, we find from Eq. (2) that the data points between the two arrows in Fig. 2 are due to protons having less than 0.26 eV of energy in the c.m. of H_3^+. For the rest of the discussion, protons having ≤ 0.26 eV of energies will be called near-zero energy protons.

Because of the finite size of the analyzer's aperture, the protons having near-zero projectile-frame energies are collected and counted more efficiently than those with high energies. This is due to the fact that protons of near-zero energy do not leave the H_3^+ beam and are collected with 100% efficiency when the detector is placed on the beam axis, as in the present case. Therefore the central peak should not be taken as the most probable process. However, the near-zero energy protons result from a set of physically interesting three-body dissociation processes. Finally, we will also present an approximate projectile-frame energy spectrum for the full distribution to further elucidate the proton production mechanisms for the collision-induced dissociation (CID) of H_3^+.

III. DISCUSSION

Assuming an isotropic projectile-frame distribution of H^+, it is possible to extract an approximate energy distribution of protons in the c.m. of the dissociating H_3^+, using the principle that the number of protons reaching the detector is independent of the reference frame in which this number is expressed. For a given energy of the protons in the laboratory frame, the ratio of the measured number of protons N to the total number of protons $N_{\text{c.m.}}$, emitted in all directions in the projectile frame, is given by the ratio of the detector's acceptance solid angle expressed in the projectile frame to 4π, i.e.,

$$N/N_{\text{c.m.}}=[1-\cos(b)]/2\ , \tag{3}$$

where b is the half-central angle of the detector's acceptance solid angle in the projectile frame. The angle b can be readily related to the half-central angle of the detector's acceptance solid angle in the laboratory frame (0.03° in our case) through a Galilean transformation of velocities. Thus each measured energy spectrum $N(E_{\text{lab}})$ can be transformed into a projectile-frame energy distribution $N_{\text{c.m.}}(\varepsilon_+)$. However, one should note here that this procedure assumes only one inelastic energy loss value Q rather than a distribution of Q values.

Figure 4 shows the above-described c.m. transformation applied to the full laboratory H^+ spectrum of Fig. 2(a). Protons moving forward (backward) in the c.m. of H_3^+ are shown by triangles (circles). A $Q=26$ eV value is used in the transformation equations. Changing Q to a different value makes the forward-backward components more asymmetric. This strongly suggests that $Q=26$ eV represents the inelastic energy loss to H_3^+ states producing near-zero energy protons. From this graph, the most probable projectile-frame energy of H^+ is determined to be approximately 4.6 eV. A polynomial fit to the transformation of data points for each set is shown by the continuous curves. The positions of the arrows of Fig. 2 that we used to separate the central peak from the Aston bands indicate a projectile-frame energy $\varepsilon_+=0.26$ eV which is also marked by an arrow in the projectile-frame energy spectrum of Fig. 4.

There are three possible but fundamentally different ways to produce a proton from the collisional dissociation of H_3^+. The first possibility is the two-body dissociation of H_3^+ into H^++H_2 where H_2 may be in its ground or excited bound state. A second possibility is the H^++H+H channel. In this channel, any H may be in its ground or excited state. Finally, there is the $H^++H^++H^-$ channel, which was the subject of our previous study.[5] By integrating the H^+ and H^-

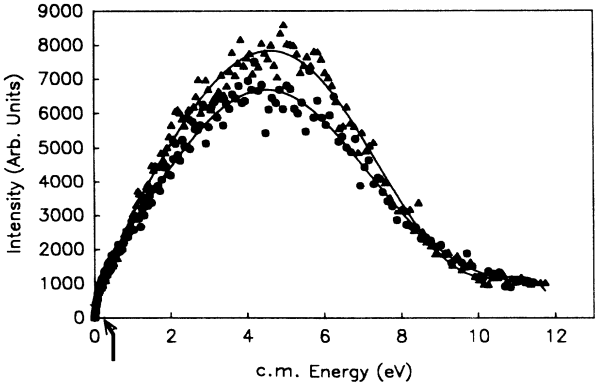

FIG. 4. Approximate projectile-frame energy distribution of H^+ obtained from the transformation of the laboratory spectrum of Fig. 2(a) to the c.m. of the projectile using the procedure described in the text. An inelastic energy loss of $Q=26$ eV is used in the transformation equations. Protons moving in the same direction as the beam are shown by triangles. Protons moving opposite to the beam direction are shown by circles. The solid lines are least-squares polynomial fits to the data for each case.

projectile-frame spectra obtained under similar conditions, we estimate that the H^- channel accounts for approximately 10% of total proton production mechanisms.

In a two-body dissociation, the momentum conservation requires that the total available kinetic energy in the c.m. of the dissociating molecule is shared by the fragments in the inverse ratio of their masses. This implies that, if the projectile-frame kinetic energy of one of the fragments is near zero, the total available kinetic energy must also be near zero. On the other hand, in the three-body dissociation, it is possible to have a fragment with near-zero projectile-frame kinetic energies even when the total available kinetic energy in the c.m. of the dissociating molecule is substantial. In that case, the extra energy is carried away by the two remaining fragments while conserving momentum.

The molecular orbitals (MO's) of the H_3^+ molecule are used to help identify the different processes that produce protons, which form the central peak or the Aston bands of the experimental laboratory proton energy distributions. The energies of the ground and 19 singly excited states of an equilateral H_3^+ (D_{2h} symmetry) have been calculated by Schaad and Hicks for both the singlets and the triplets using a basis set of s and p Gaussian orbitals.[10] A more recent calculation of Talbi and Saxon[11] reports the 13 lowest singlet states in C_{2v} (isosceles) symmetries. Since the incoming H_3^+ is in an equilateral triangle form, the energy curves in D_{3h} symmetry have to be used to describe the excitation of the molecule during the collision. Figure 5 shows the singlet H_3^+ energy curves and the first triplet $1\,^3E'$ in D_{3h} symmetry as calculated by Schaad and Hicks[10] as a function of the distance R between the protons in an equilateral triangle

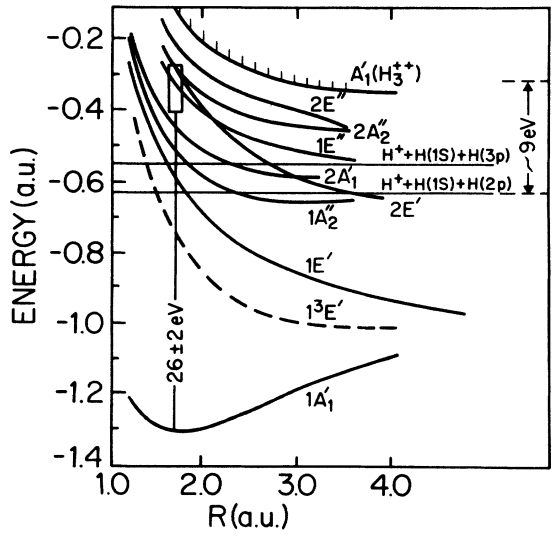

FIG. 5. The energies of the first eight singlets (solid lines) and the first triplet (dashed line) of H_3^+ in D_{3h} symmetry, as calculated by Schaad and Hicks (Ref. 10), as a function of the distance R between the protons forming an equilateral triangle. The measured inelastic energy loss of 26±2 eV is shown by the vertical transition.

configuration. After excitation, the D_{3h} states may branch into several dissociation channels of different symmetry. For some dissociation paths, the D_{3h} degeneracies of the energy curves are removed. For completeness, we reproduced in Fig. 6 the correlation diagram connecting the D_{3h} states of H_3^+ to its two-body or three-body dissociation asymptotes as given by Talbi and Saxon.[11] We also indicate in Fig. 6 the energy difference between the D_{3h} states and their dissociation limits for the Franck-Condon region of the vibrational ground state of $1\,^1A_1'$.

The measured inelastic energy loss $Q=26\pm2$ eV for protons with near-zero projectile-frame energies can be accounted for by two different excitation mechanisms. The first possibility is that the low projectile-frame energy protons are produced by a singlet excitation of H_3^+ to a distribution of $2\,^1E'$, $1\,^1E''$, and $2\,^1A_2''$ states. Figure 6 indicates the possible two- or three-body dissociation limits of these states along with the maximum and minimum energy available above the dissociation limits. From Fig. 6, we find for the two-body dissociation of H_3^+ into $H^+ + (H_2)^*$ that the total available kinetic energy to be shared by the fragments varies from 3.4 to 12 eV depending on the initial states of H_3^+ that are excited and their final dissociation limits. Therefore protons having near-zero projectile-frame kinetic energies cannot be produced by a two-body dissociation since the linear momentum has to be conserved in the c.m. of the dissociating molecule.

The second possibility is the triplet excitations of H_3^+. When spin-orbit interactions between the collision partners are weak, the direct excitation of triplets is less probable. Because of the Wigner spin rule,[12] the only other way to have a triplet excitation of H_3^+ is to have an electron exchange between H_3^+ and He. Such a process would leave He excited with 20 eV of energy and $(H_3^+)^*$ with 6 eV of internal energy. Then, we note from the energy curves of H_3^+, the only possible excitation of H_3^+ would be to the $1\,^3E'(1a_1'1e')$ state at an internuclear distance of approximately 2.75 a.u. In analogy with the singlet correlations presented in Fig. 6, the two-body dissociation limits of $1\,^3E'$ are $H^+ + H_2(b\,^3\Sigma_u^+)2p\sigma$ and $H_2^+(X\,^2\Sigma_g^+) + H(1s)$. The first dissociation is not energetically possible if the transition to $1\,^3E'$ state is near $R=2.75$ a.u. The second channel does not produce a proton. Thus the only remaining possibility is the three-body dissociation of $1\,^3E'$ state into $H^+ + H(1s) + H(1s)$. In this case, the internal energy above the dissociation limit is almost zero and all the fragments are produced with near-zero projectile-frame energies.

Thus protons with near-zero projectile-frame kinetic energies have to be produced by a *three-body* dissociation of $(H_3^+)^*$. If the excitation is to $1\,^3E'$, then the near-zero projectile-frame protons are produced by the dissociation of this state into $H^+ + H(1s) + H(1s)$. In the case of a singlet excitation, the dissociation produces $H^+ + H(1s) + H^*$. From the correlation diagram Fig. 6, the excited H atom can be either in $H^*(n=2)$ or $H^*(n=3)$ states. Our experimental resolution does not allow us to make any assessment of the relative populations of

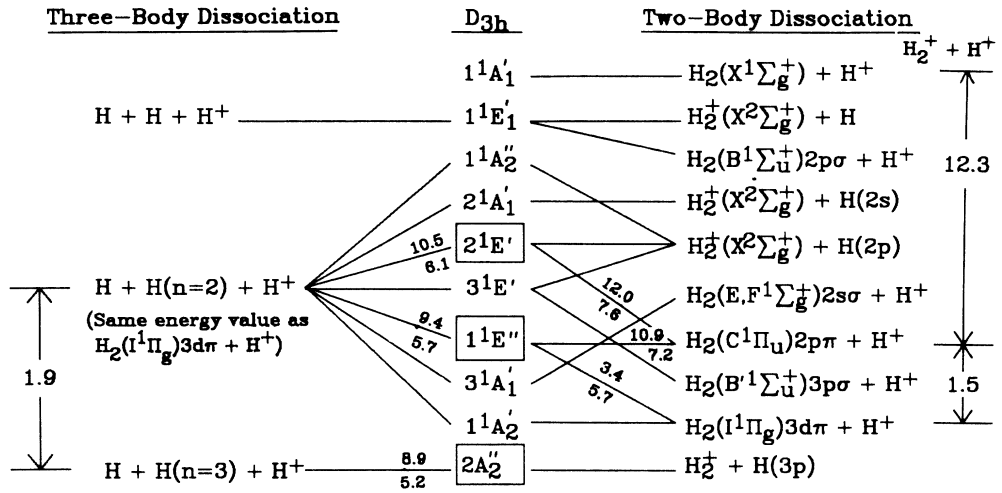

FIG. 6. Correlation diagram connecting the D_{3h} states of H_3^+ to their two-body or three-body dissociation asymptotes as given by Talbi and Saxon (Ref. 11). The excited states of H_3^+ corresponding to a $Q=26\pm2$ eV value are boxed. Assuming a Franck-Condon transition from the lowest vibrational level of the electronic ground state to the excited D_{3h} state, the maximum available internal energy to be shared by the dissociation fragments is shown by the upper number. Similarly, the lower number is the minimum available internal energy that has to be shared by the dissociation products under the same assumptions.

$H^*(n=2)$ or $H^*(n=3)$.

The kinetic energy of the fragments in the c.m. of H_3^+ is provided by the internal energy of $(H_3^+)^*$ before the dissociation. For the triplet excitation, the internal energy of $H_3^+(1\,^3E')^*$ is small and all fragments have near-zero energies in the c.m. of H_3^+. For the three-body dissociation of $2\,^1E'$, $1\,^1E''$, and $2\,^1A_2''$, this extra energy is approximately 5.5–10.5 eV depending which one of the above-mentioned states is excited and the internuclear separation between the nuclei at the moment of excitation. For the central peak, we have mentioned that approximately 0.26 eV (or less) is carried away by the proton. The remaining energy is shared by the two neutral H atoms which move in the H_3^+ c.m. with an angle θ_{12} that will be called the correlation angle (refer to Fig. 3). For these three-body dissociations, the energy and momentum conservation is not sufficient to determine what the correlation angle is and how the extra kinetic energy is shared by the two H atoms. However, one can calculate the correlation angle θ_{12} as a function of the relative kinetic energies of the fragments for a given total available internal energy. In Fig. 7, we show a three-dimensional surface θ_{12} as a function of the energy ε_+ of the proton and the energy ε_0 of one of the neutral H atoms. For the graph presented, the total available kinetic energy shared by the fragments is 9.2 eV. This is the available kinetic energy from the dissociation of $H_3^+(2\,^1E')^*$ into $H^+ + H(1s) + H(n=2)$ at the equilibrium separation of H_3^+. When one uses the dissociation energies of $1\,^1E'$ (≈ 8 eV) or $2\,^1A_2''$ (≈ 7 eV), the three-dimensional plot of Fig. 7 remains approximately the same. The surface shown reveals that the correlation angle values are 170°–180° when the protons have near-zero kinetic energies in the c.m. of H_3^+.

One should also note that the linear momentum conservation forbids extreme energy sharing schemes by the neutrals, i.e., configurations such as one neutral carrying away a large proportion of the available energy and the other having very small energies. We should emphasize here that Fig. 7 shows only the possible correlation angle values and does not make any statement about how probable any possible value is.

Thus a consistent picture emerges to describe the proton production in H_3^+-He collisions at low-keV energies. During the collision, a single-electron electronic excitation populates a distribution of $2\,^1E'$, $1\,^1E''$, or $2\,^1A_2''$

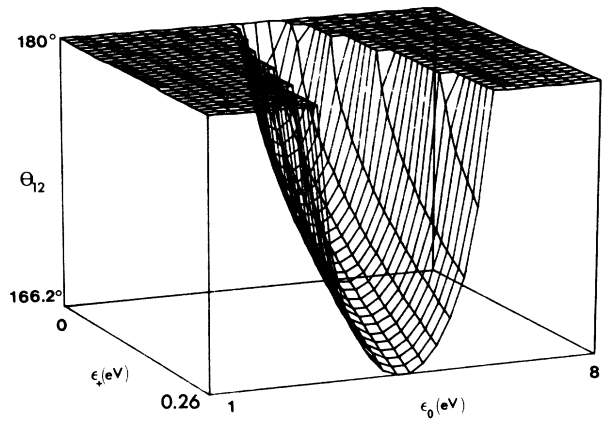

FIG. 7. Dependence of the correlation angle θ_{12} between the neutral atoms (refer to Fig. 3) as a function of the energies ε_+ of the proton and ε_0 of one of the neutral H atoms. The total available kinetic energy to be shared by the three fragments is 9.2 eV. Notice that extreme energy sharing schemes, i.e., configurations such as one neutral carrying away a large proportion of the available energy while the other neutral having small energies, are forbidden by the linear momentum conservation.

states, or as an alternative, $1\,^3E'$ with a simultaneous excitation of the He target. Our earlier works on H_3^+ suggest[5,13] that the triplet excitation is less likely since the incoming H_3^+ is mostly in the ground vibrational state. Nevertheless, in either case, near-zero kinetic energy protons in the c.m. of H_3^+ are produced by a three-body dissociation of $(H_3^+)^*$. The remaining portion of the laboratory distribution is obtained by a combination of two- and three-body dissociations.

The above-described picture is also consistent with our previously measured Ly-α studies.[13] From the correlation diagram of Fig. 7, one of the two-body dissociation limits of $2E'$ excited state is $H_2^+ + H(2p_0, 2s)$ for which we have measured the polarization of Ly-α radiation in coincidence with the H_2^+.[13] An excitation mechanism of this state, based on the qualitative quasidiatomic model, was presented in Ref. 13.

IV. CONCLUSION

This paper addresses two fundamental questions. The first part deals with the measurement of the laboratory proton energy spectrum from the dissociation of H_3^+ and the identification of the excited states of H_3^+ which produce the observed low projectile-frame energy protons. The second component uses H_3^+ dissociation as a tool to study the three-body problem.

The results that we presented above suggest that the principal mechanisms for producing protons with near-zero projectile-frame energies are either the single-electron excitation of the H_3^+ ground state to a distribution of $2\,^1E'$, $1\,^1E''$, or $2\,^1A_2''$ states accompanied by their subsequent three-body dissociation into $H^+ + H(1s) + H^*$, or the simultaneous triplet excitations of the He target and $H_3^+(1\,^3E')^*$ which dissociate into $H^+ + H(1s) + H(1s)$. Higher-energy protons forming the Aston bands are due to both three- and two-body mechanisms.

The interpretation of the three-body dissociation of H_3^+ is a little more involved. First, we have to remember that an inelastic cross section is the product of a squared matrix element (that we will call the dynamical term) and a phase space factor due to the density of states (that we will call the kinematical term). In the case of two-body final states, Wigner showed that, in the absence of long-range forces, the energy dependence of the cross section near the threshold is determined by the kinematical term.[14] In order to determine whether long-range interactions are present, for two-body interactions one has to compare the kinematical angular momentum term $L(L+1)/2\mu r^2$ where r is the relative coordinate between the two particles, with the r dependence of the interaction. For any interaction which goes to zero faster than $1/r^2$, the energy dependence of the cross section at threshold is obtained from the density of states alone and the energy dependence of the matrix element is negligible.

In the case of the three-body interactions, one uses the hyperspherical radius R to describe the system. Following Klar,[3] the hyperspherical radius R can be defined in terms of the interparticle distances r_{ij},

$$m_0 M R^2 = \sum_{i<j} m_i m_j r_{ij}^2 , \tag{4}$$

where m_i denotes the mass of the ith particle and M is the total mass of the particles. If m_0 is taken to be the electron's mass, then all distances are expressed in terms of atomic units. To be consistent with Fig. 3, the subscripts 1, 2, and 3 denote H($1s$), H($2p$), and H^+, respectively. The Hamiltonian of such a system outside of the reaction zone[3,15] is

$$H = -\frac{1}{2} R^{-5} \frac{\partial}{\partial R} R^5 \frac{\partial}{\partial R} + \frac{\Lambda^2}{2R^2} + V(\mathbf{r}) , \tag{5}$$

where Λ is the grand angular momentum and $V(\mathbf{r})$ the total interaction potential. Note that in the case of Coulomb interaction among the particles, Wannier[1] called this zone "the Coulomb zone."

In order to determine to what degree the reaction forces can be considered long range, one has to compare the relative strength of $\Lambda^2/2R^2$, the generalized angular momentum term, with the strength of the potential in the region outside of the reaction zone. In our case, in the region outside of the reaction zone, the electric field of the proton polarizes the neutral H atoms. For the singlet excitation, the final state is $H^+ + H^*(n=2 \text{ or } 3) + H(1s)$. In this case, the interaction potential between H^+ and H^* is proportional to $1/r_{23}^2$ (first-order Stark effect). Similarly, the interaction between H^+ and H($1s$) is proportional to $1/r_{13}^4$ (second-order Stark effect). Finally, H^* and H($1s$) interact through an induced dipole-dipole interaction proportional to $1/r_{12}^3$. Thus the total potential becomes

$$V(r) = -A/r_{23}^2 - B/r_{13}^4 + C/r_{12}^3 , \tag{6}$$

where A, B, and C are constants depending on the induced dipole moments. The generalized angular momentum term in Eq. (5), expressed in terms of the interparticle distances, is

$$\Lambda^2/2R^2 = \tfrac{1}{2} M m_0 \Lambda^2 (m_1 m_2 r_{12}^2 + m_1 m_3 r_{13}^2 + m_2 m_3 r_{23}^2)^{-1} . \tag{7}$$

Since our experimental results suggest that the low-energy protons are produced by a three-body process, in the region outside of the reaction zone, r_{ij} values, for all i and j, are large (no two particles are bound). Although the potential terms containing r_{13} and r_{12} go to zero faster than the grand angular momentum term, the A/r_{23}^2 term ensures that the potential remains comparable to the kinematical term. Thus the threshold energy dependence of the cross section to produce low-energy protons in the c.m. of the dissociating H_3^+ cannot be determined alone from the density of states factor. One has to include the dynamical term, i.e., the interaction matrix between the initial and final states, causing departures from the Wigner law.

When the triplet state is excited, the final dissociation channel is $H^+ + H(1s) + H(1s)$. In this case, the electric field of the proton interacts with the induced dipole of each ground-state hydrogen atom through a potential proportional to $1/r_{ij}^4$. The dipole-dipole interaction be-

tween the two H(1s) is still proportional to $1/r_{12}^3$. Thus the energy dependence of the collision cross sections at threshold do not depend on the dynamics since the long-range interactions between the fragments vanish faster than the kinematical term, which is proportional to $1/R^2$.

In the case of the singlet excitation of H_3^+, the long-range part of the potential is due to the production of an excited H* atom upon dissociation, which gives rise to the dynamical energy dependence at threshold of the cross section. Only in this case is the motion of the two neutrals correlated, the angle between them being limited by the energy carried away by the H^+, as shown in Fig. 7.

The attractive interaction between the electric field of the H^+ and the induced dipoles of the H and H* is the origin of the force which slows down the proton. The induced, repulsive dipole-dipole interaction between the neutral H atoms provides the force that makes the correlation angle θ_{12} close to 180°. Our experimental results are consistent with this description.

ACKNOWLEDGMENTS

We would like to thank Dr. M. Cavagnero for important comments and stimulating discussions. The support of this work by the National Science Foundation through Grant No. PHY-8701905 is gratefully acknowledged.

[1]G. H. Wannier, Phys. Rev. **90**, 817 (1953).
[2]J. Mazeau, A. Huetz, and P. Selles, in *Invited Papers of the Fourteenth International Conference on the Physics of Electronic and Atomic Collisions, 1985,* edited by D. C. Lorents, W. E. Meyerhof, and J. R. Peterson (North-Holland, Amsterdam, 1986), p. 141.
[3]H. Klar, Z. Phys. A **307**, 75 (1982).
[4]J. M. Feagin, J. Phys. B **17**, 2433 (1984).
[5]O. Yenen, D. H. Jaecks, and L. M. Wiese, Phys. Rev. A **39**, 1767 (1989).
[6]R. G. Cooks and J. H. Beynon, Chem. Commun. **98**, 1282 (1971).
[7]G. Lange, B. Huber, and K. Wiesemann, Z. Phys. A **281**, 21 (1977).
[8]B. Meierjohann and M. Vogler, Z. Phys. A **282**, 7 (1977).
[9]W. Baldreich, W. W. Lotz, and H. Ewald, Z. Phys. A **317**, 23 (1984).
[10]L. J. Schaad and W. V. Hicks, J. Chem. Phys. **61**, 1934 (1974).
[11]D. Talbi and R. P. Saxon, J. Chem. Phys. **89**, 2235 (1989).
[12]J. H. Moore, Jr., Phys. Rev. A **8**, 2359 (1973); **10**, 724 (1974).
[13]O. Yenen and D. H. Jaecks, Phys. Rev. A **32**, 836 (1985).
[14]E. P. Wigner, Phys. Rev. **73**, 1002 (1948).
[15]H. Mayer, J. Phys. A **8**, 1562 (1975).